JOINED-WING CONFIGURATION AERODYNAMICS

Wai, J. C., Herling, W.W., and Roetman, E. L.
Boeing Defense and Space Group
Seattle, Washington

Abstract

The three-dimensional, thin-layer, Navier-Stokes code, OVERFLOW, with Chimera overset grid topology and the full potential TRANAIR code have been applied to an analysis of a joined-wing configuration. Solutions are presented for subsonic Mach number, yawed conditions. Analysis is compared with wind tunnel results obtained in the NASA/LaRC 16-foot transonic and Microcraft low speed wind tunnels at low subsonic conditions. Comparisons of predicted surface flow patterns, force and moments, and surface pressure distributions from the analysis are made with the experimental data. The degree of agreement is dependent on modeling approach and test condition.

Introduction

Boeing is developing a joined-wing aircraft as a carrier-based reconnaissance platform. The primary purpose of this study is to assess the computational fluid dynamics (CFD) technology required to support the design of this aircraft. Figure 1 shows the layout of this configuration. The aircraft shape was determined by the arrangement of the antennae planform contained within the wing surfaces. This unique arrangement raises an important issue: how to model this complex configuration while capturing the flow physics of multiple, thick lifting surfaces in close proximity. In particular, an assessment of the accuracy of CFD techniques in predicting lateral/directional characteristics is needed.

An initial design approach used for the wing design of the configuration relied on a combination of linear design methods for overall configuration design and inviscid, non-linear design optimization techniques for the design of individual wing panels. This design was tested in cooperation with NASA/LaRC in their 16-foot transonic wind tunnel in 1993. This model was instrumented with static pressure orifices on the wing surface to provide a data base to facilitate validation of CFD codes. A low speed test was performed recently in the Microcraft wind tunnel in 1995 with a second wing design. In this paper, the application of a Navier-Stokes code and full potential code to analysis of this joined-wing configuration with comparison to test data is presented.

Several options are currently available for the analysis of complex configurations. These include panel methods, Cartesian grid methods, unstructured grid methods, and overset grid methods. Each has their distinct advantages and disadvantages mainly involving computational resources required and corresponding solution accuracy's. Overset, structured grid generation schemes provide great flexibility to model complex configurations with Navier-Stokes level physics but at the cost of significant computational resources. In contrast, solution techniques using Cartesian grid technology provide rapid means to model very complex geometric details but have yet to be demonstrated for complex flow fields. In previous work reported by the authors (ref. 1), overset, unstructured and panel methods were compared for this configuration at transonic, zero yaw conditions. In the work presented here, computations are compared from the NASA/Ames OVERFLOW code (ref. 2) using overset grids with those from the TRANAIR code (ref. 3), a full potential solver using Cartesian grids.

Chimera Grid Generation

The structured grid generation of the joined-wing configuration was generated with the Chimera overlapped grid scheme. The Chimera scheme simplifies complex geometry domain decomposition by allowing structured body-fitted grids to be generated for separate components of the aircraft. Interpolation stencils are set up to communicate boundary information at the interface between separate zones and overlapped regions. Holes are cut in grids that intersect solid bodies.

Figure 1 shows the surface grid arrangement using the Chimera topology for the fuselage and wing alone geometry. The fuselage geometry was modeled as tested in the wind tunnel set up with a sting shield partially covering the aft portion of the fuselage, and a sting mount extending downstream. For viscous flow computations about intersecting pieces of geometry such as the wing and fuselage, juncture of fore and aft wings, and aft wing and vertical tail, generation of suitable grids to capture the correct physics becomes an

important issue. The approach used in the present analysis follows the collar grid method developed in ref. 4. Collar grids are used to connect related component grids in the intersection region and grid density is increased to capture the viscous flow physics in the corners. The collar grids used are highlighted in Figure 1.

Figure 2 shows a close up view of the collar grid used in the juncture region for connecting the fore/aft wings and wing tip. The basic components consist of three standard C-grid meshes. The fore and aft wing grids are blended together and folded over to connect to the wing tip topology. This collar grid enables the construction of viscous grids to simulate the boundary-layer over the face on the inboard edge of the wing tip between the two wing planforms. The C-grid wake sections used for connecting the fore and aft wings and behind the trailing edge were removed in this figure for clarity. The contribution of this collar grid is to enable the viscous flow over three different components to be computed within a single block. At the edge of the wing tip, two different grid topologies had been used. The simple approach was to extend the wing tip to form a C-slit wake-like grid extending spanwise from the tip. This grid arrangement was found to produce inaccuracies as a consequence of the thick airfoil section used in this configuration. The second approach used a wing tip cap to form a cover to enclose the side edge on the wing tip as shown in Figure 2, providing greater geometric fidelity of the tip region. This arrangement allows a better representation of the viscous flow phenomena in the rapidly changing flow field near the wing tip region.

The 3-D grid for each individual block was constructed with the hyperbolic grid generation code of ref. 5. Nineteen blocks of mesh were used to construct the fuselage/wing planform geometry, with an addition of four blocks to represent the wind tunnel sting assembly and two blocks of global grid to cover the entire computational domain. The selection of grid spacing and dimensions was biased towards the normal directions for the purpose of capturing a good viscous flow. Grid densities were chosen to ensure a sufficient resolution of the viscous flow physics. A total of 19 million mesh points were used to simulate a full configuration at yawed condition. The analysis was carried out on CRAY C-90 computers.

Navier-Stokes Flow Solver

The Navier-Stokes flow solver used in the viscous flow analysis is known as the OVERFLOW code developed by NASA/Ames Research Center (ref. 2). This code uses an implicit diagonalized approximate factorization algorithm to solve the thin-layer formulation of the Navier-Stokes equations. The algorithm uses a central differencing scheme with added second and fourth-order artificial dissipation. This code processes the accounting information of Chimera overset grids and runs with a local time-step to accelerate the convergence rate. OVERFLOW cycles through the grids one at a time, advances the solution for the current grid and communicates updated flow field information in the overlapped regions to other grids.

For viscous flow simulation used in the present study, two different one-equation turbulent models were used. The first model was developed by Baldwin-Barth (ref. 6). This model is based on a simplification of the K-ε turbulence equations and formulated to solve a field equation for the turbulence Reynolds number. The advantage of this model as compared with algebraic models is the removal of the length scale prescription. For a complex geometry such as the joined-wing configuration, this model simplifies the set up required for turbulent calculations. This model performs reasonably well in attached flow regions and converges to a smooth distribution of turbulent eddy viscosity across overset grid boundaries (ref. 7). The second model used was that developed by Spalart-Allmaras (ref. 8). The derivation of this model was constructed on empirical reasoning and dimensional analysis, where empirical constants have been calibrated to capture turbulent flow characteristics. This model has become a popular technique to predict flows with mild separation due to its treatment of wake type flow.

TRANAIR flow potential flow solver

In contrast to the relatively involved grid generation process for overset grids, geometry's are modeled in TRANAIR using network of flat panels, with curvature simulated by linearly varying normals. The Cartesian grid generation proceeds automatically within a computational domain defined by a uniform global grid. This grid is refined locally in a solution adaptive procedure near the surface and in areas of increased flow gradients. Figure 3 shows the resulting TRANAIR grids used for the joined-wing configuration. A total of 800,000 cells or boxes with refinement to

four sub-levels were used to produce a finite element solution to the full potential equation. The solution process includes grid sequencing for

convergence acceleration and special treatment of boundary conditions at the edge of the global grid to further reduce the spatial extent of the computational domain. It is possible to capture viscous effects through the use of coupled boundary layer solvers, either a finite difference method or an integral method. Evaluation of these viscous methods applied to the joined-wing configuration are currently in work. The work reported below addresses only the inviscid solution process. All computations were completed on workstation class computers.

Results and discussions

The OVERFLOW code with the Baldwin-Barth turbulence model was evaluated for the partial geometry of Figure 1 consisting of the vertical tail and the fuselage without the sponson associated with the forward wing juncture. The computational grids used were a subset of the grids used for the complete configuration. The experimental test was performed in the Microcraft 8 ft x 12 ft low speed wind tunnel at Mach number 0.18 and 5 degree yaw angle. Figure 4 shows the force and moment comparisons between the experiment and computation. The lift, drag and pitching moment are in good agreement with the experiment. At higher angles of attack, the flow is separated near the aft portion of the fuselage. as a result, the comparison in side force, yaw and roll moments are less accurate. In general, the data demonstrates that the computation approach used has the capability to reproduce the overall experimental distributions.

The full configuration was tested in the NASA/LaRC 16-foot wind tunnel using a scaled 1/10 model at Mach 0.30. The test condition corresponds to a unit Reynolds number of 1.9 million per foot. As with the test above, this model was also mounted with a sting support entering the aft end of the fuselage. A series of streamwise pressure orifices were mounted at different spanwise locations on the fore and aft wings, wing tip and the vertical fin. Oil flow visualization was also obtained during the wind tunnel test.

The computed surface flow patterns from the viscous flow analysis using OVERFLOW and Baldwin-Barth turbulence model for the complete configuration are shown in Figure 5 at 10 degree angle of attack and 5 degree yaw angle. The separation pattern on the wing tip region was mainly influenced by the cross flow separation initiated on the fore wing and the adverse pressure condition at the juncture of the fore and aft wings. It is postulated that due to the incidence of the aft wing, a crossflow separation is produced by the juncture flow between the aft wing and the vertical fin. An experimental flow visualization was not taken at this same flow condition. The closest available oil flow pattern as shown in Figure 6 was obtained at Mach number 0.38, 4 degree angle of attack and 0 degree yaw angle. The major flow characteristics are essentially the same, indicating a strong cross flow separation pattern.

Figure 7 shows the comparison of the forces and moments for the complete configuration at Mach number 0.30 and 5 degree yaw angle. The computed results from OVERFLOW with the two different turbulence models and TRANAIR are shown. For the viscous calculations, the predicted results are very similar, indicating that the difference in the two turbulence models are minor. In the course of this study, the fuselage was originally modeled without the wind tunnel sting mount support. Results from this simulation shows poor agreement with the side force and yaw moment comparison. The next approach includes the sting mount and a simple wake slit to model the wing tip as described earlier. These results improve the agreement slightly. Both of these historical results are included in the comparison shown in Figure 7. When the configuration was modeled more accurately in the wing tip region, the OVERFLOW code reproduces the overall trend in the forces and moments. The TRANAIR results give a much larger discrepancy. The severe flow nature of this configuration with separated flow is beyond the simulation limit of TRANAIR. The degree to which these viscous effects can be captured with coupled boundary layer techniques remains an open issue.

Predicted surface pressures are compared with the experiment in Figure 8 for Mach number 0.30, 5 degree angle of attack and 5 degree yaw angle. The experimental results were obtained at the nearest nominal yaw angle to that used in the computation. The pressure orifices provide data for the leeward side comparison only. The OVERFLOW analysis with the two different turbulence models show similar agreement with the experiment. The severe flow characteristics at the wing tip beyond the wing juncture were predicted. The higher pressure at the trailing edge from the TRANAIR results indicate the importance

of viscous, separated flow regions which are not reproduced with an invisid analysis code.

Summary

The purpose of this study was to assess the capability of CFD to support complex airplane design requirements. A complex joined-wing configuration was analyzed with the Navier-Stokes Chimera/OVERFLOW code and inviscid TRANAIR full potential code. Analysis to experimental data comparisons were performed at a subsonic Mach number for yawed conditions with severe flow condition where extensive separated regions were present on the wing surfaces. The viscous flow analysis provided good agreement with the flow physics both in terms of surface pressures, flow orientation and forces and moments data. The difference in the Baldwin-Barth and Spalart-Allmaras turbulence models are very minor in the overall comparison. The geometry modeling requirement needs to be very accurate to reproduce good yaw/roll moments and side force comparison. Complex physics is affecting TRANAIR results for a viscous flow dominated configuration.

Acknowledgments

The authors would like to thank Mr. William M. Eldridge for providing the comparison with the Microcraft test. We also like to thank NASA/Ames, USAE Waterways Experimental Station and NAVOCEANO for providing the CRAY C90 computing resources, and NASA/LaRC for the wind tunnel test time.

References

1. Wai, J.C., Herling, W.W., and Muilenburg, D.A., "Analysis of a Joined-Wing Configuration", AIAA 94-0657.

2. Buning, P.G., Chan, W.M., Renze, K.J., Sondak, D.L., Chiu, I.T., Slotnick, J.P., Gomez, R.J., Jespersen, D.C., Krist, S.E. and Rizk, Y.K., 'OVERFLOW User's Manual, Version 1.6bc", NASA Ames Research Center, Moffett Field, CA, November 1995.

3. Young, D.P., Melvin, R.G., Bieterman, M.B., Johnson, F.T., Samant, S.S. and Bussoletti, J.E., "A locally Refined Rectangular Grid Finite Element Method: Application to Computational Fluid Dynamics and Computational Physics," Journal of Computational Physics, Vol. 92, No. 1, 1991, pp. 1-66.

4. Parks, S.J., Buning, P.G., Steger, J.L., and Chan, W.M., "Collar Grids for Intersecting Geometric Components within the Chimera Overlapped Grid Scheme", AIAA 91-1587.

5. Chan, W.M., Chiu, I.T. and Buning, P.G., "User's Manual for the HYPGEN Hyperbolic Grid Generator and the HGUI Graphic User Interface", NASA Technical memorandum 108791.

6. Baldwin, B.S. and Barth, T.J., "A One-Equation Turbulence Transport Model fro High Reynolds Number Wall-Bounded Flows", AIAA 91-610.

7. Renze, K.J., Buning, P.G., and Rajagopalan, R.G., "A Comparative Study of Turbulence Models for Overset Grids", AIAA 2-437.

8. Spalart, P.R. and Allmaras, S.R., "A One-Equation Turbulence Model for Aerodynamic Flow, "AIAA 92-0439.

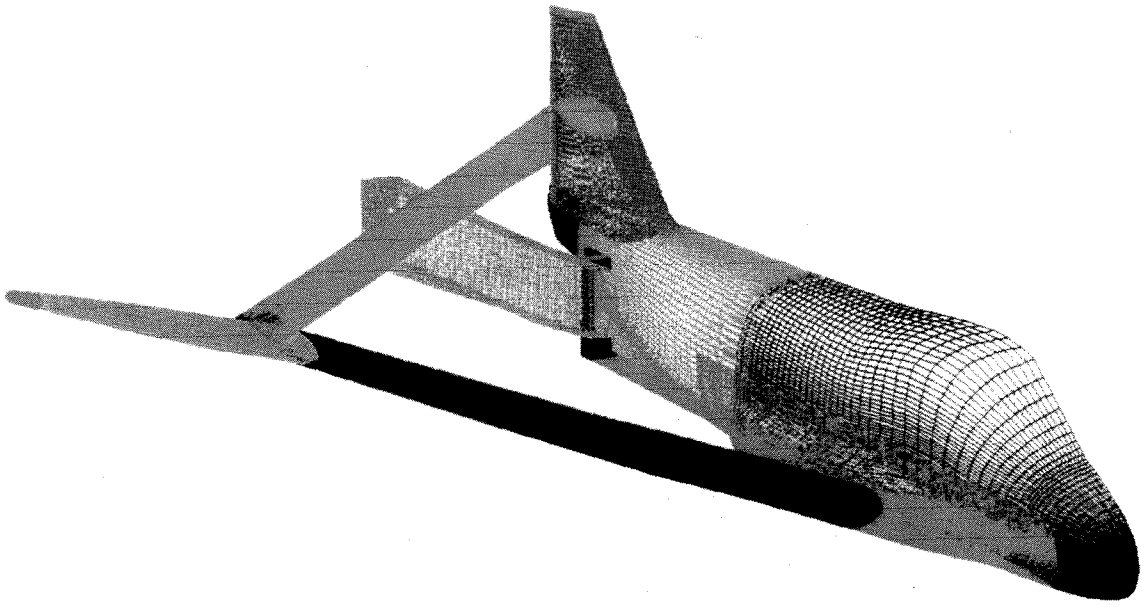

Figure 1. Chimera Grid System of a Joined-Wing Configuration

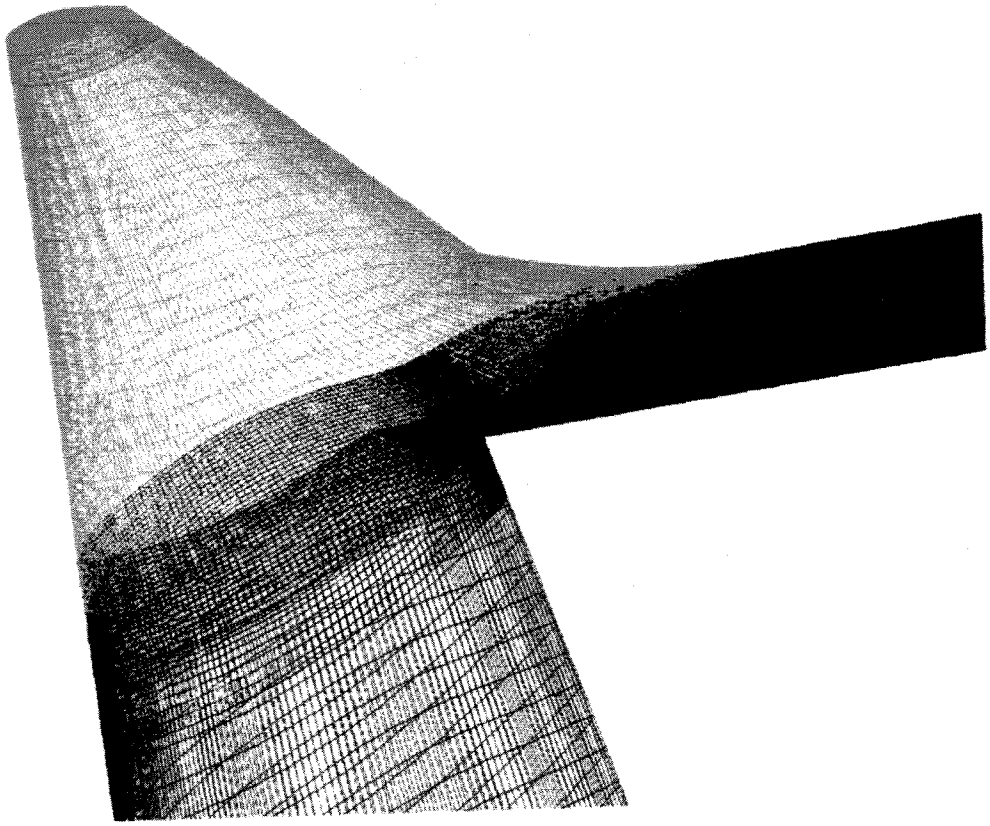

Figure 2. Collar Grid of the Joined-Wing Juncture

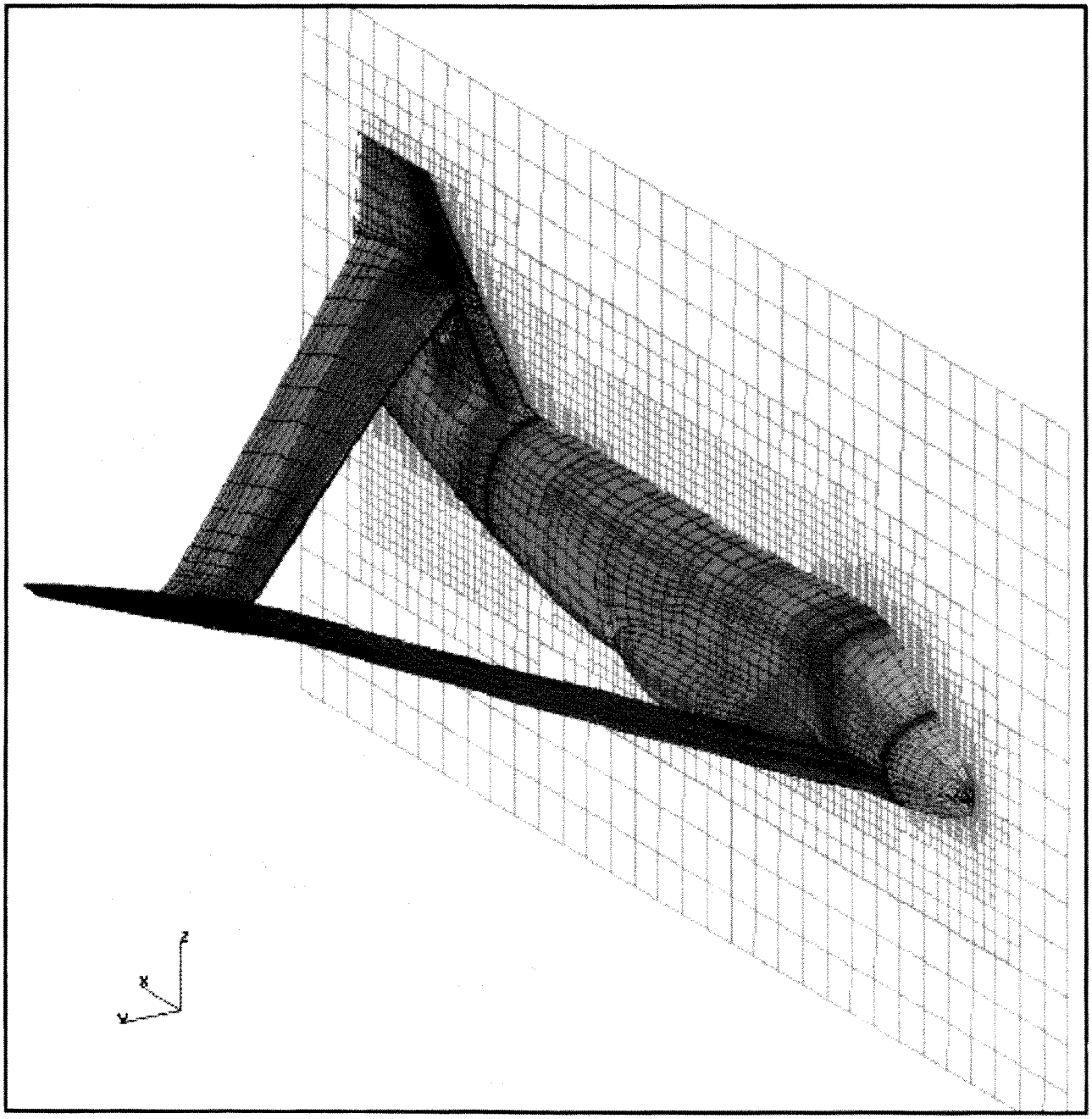

Figure 3. TRANAIR Grid of a Joined-Wing Configuration

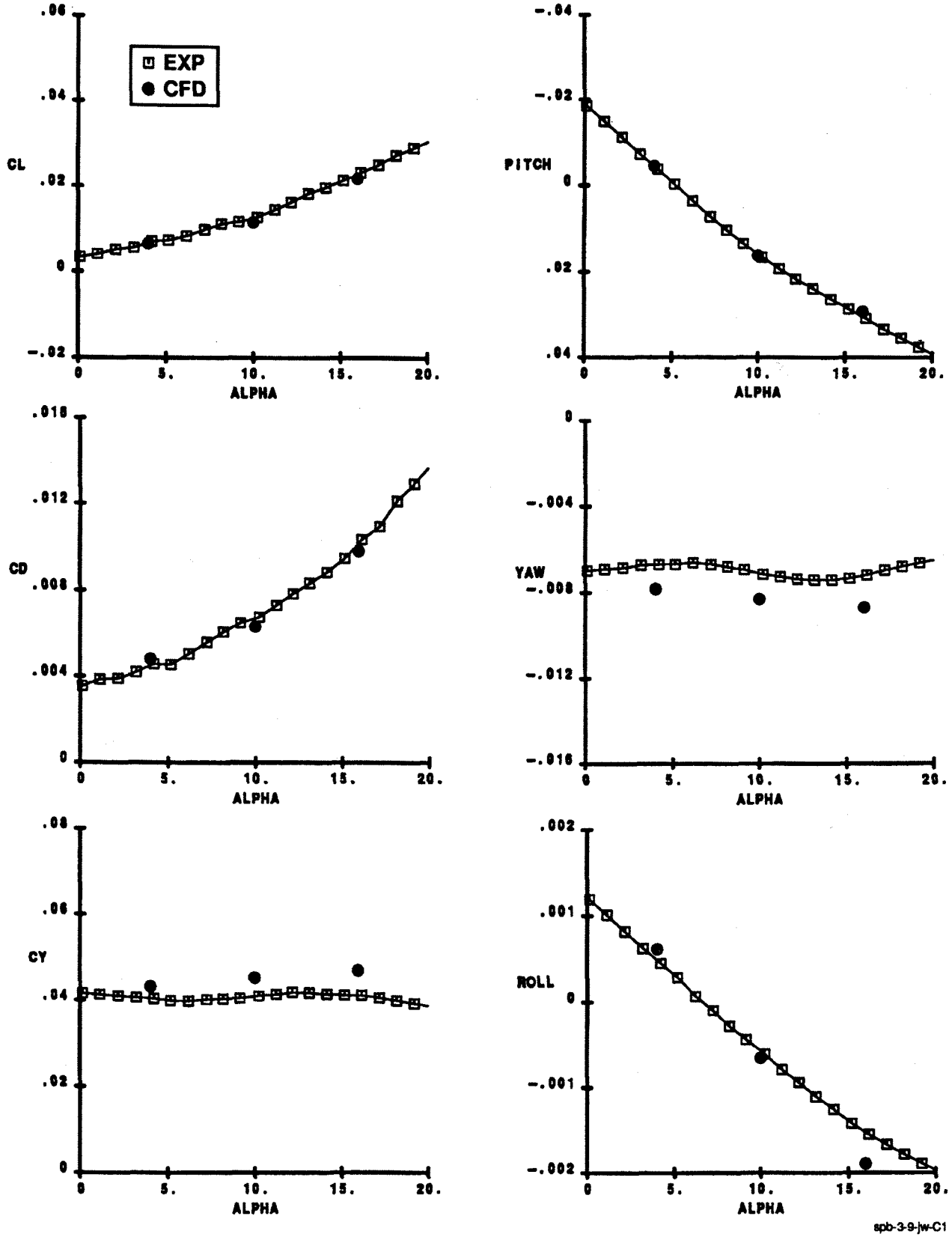

Figure 4. Forces and Moments Comparison of Fuselage at $M_\infty = 0.18$ and $\beta = 5°$

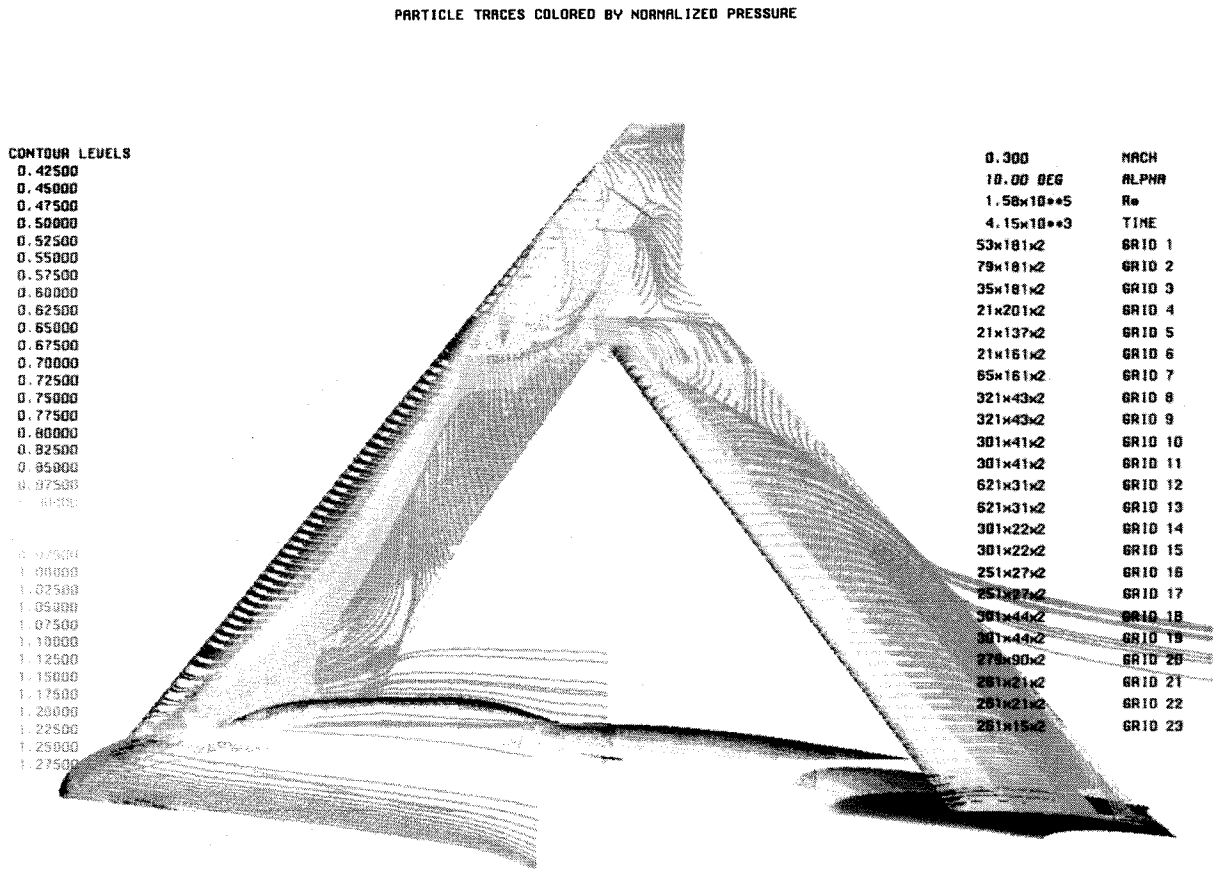

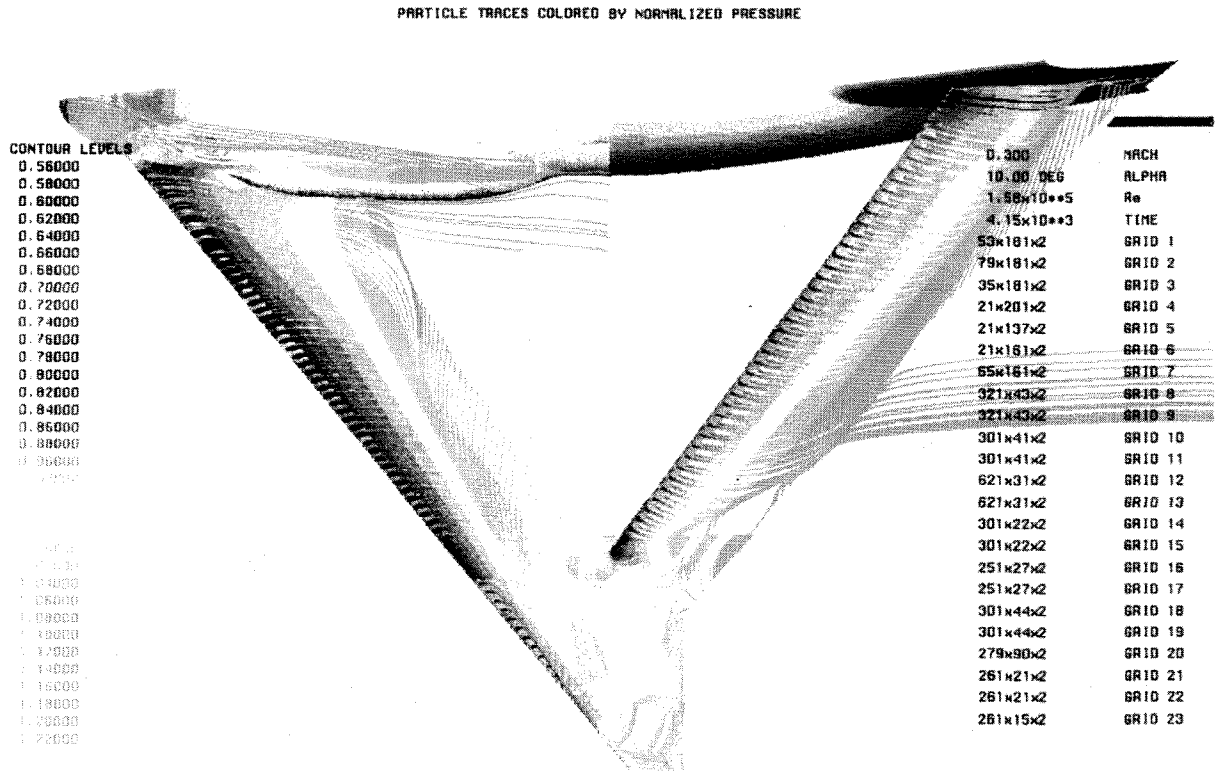

Figure 5. Predicted Surface Flow Pattern at $M_\infty = 0.3$, $\alpha = 10°$, and $\beta = 5°$

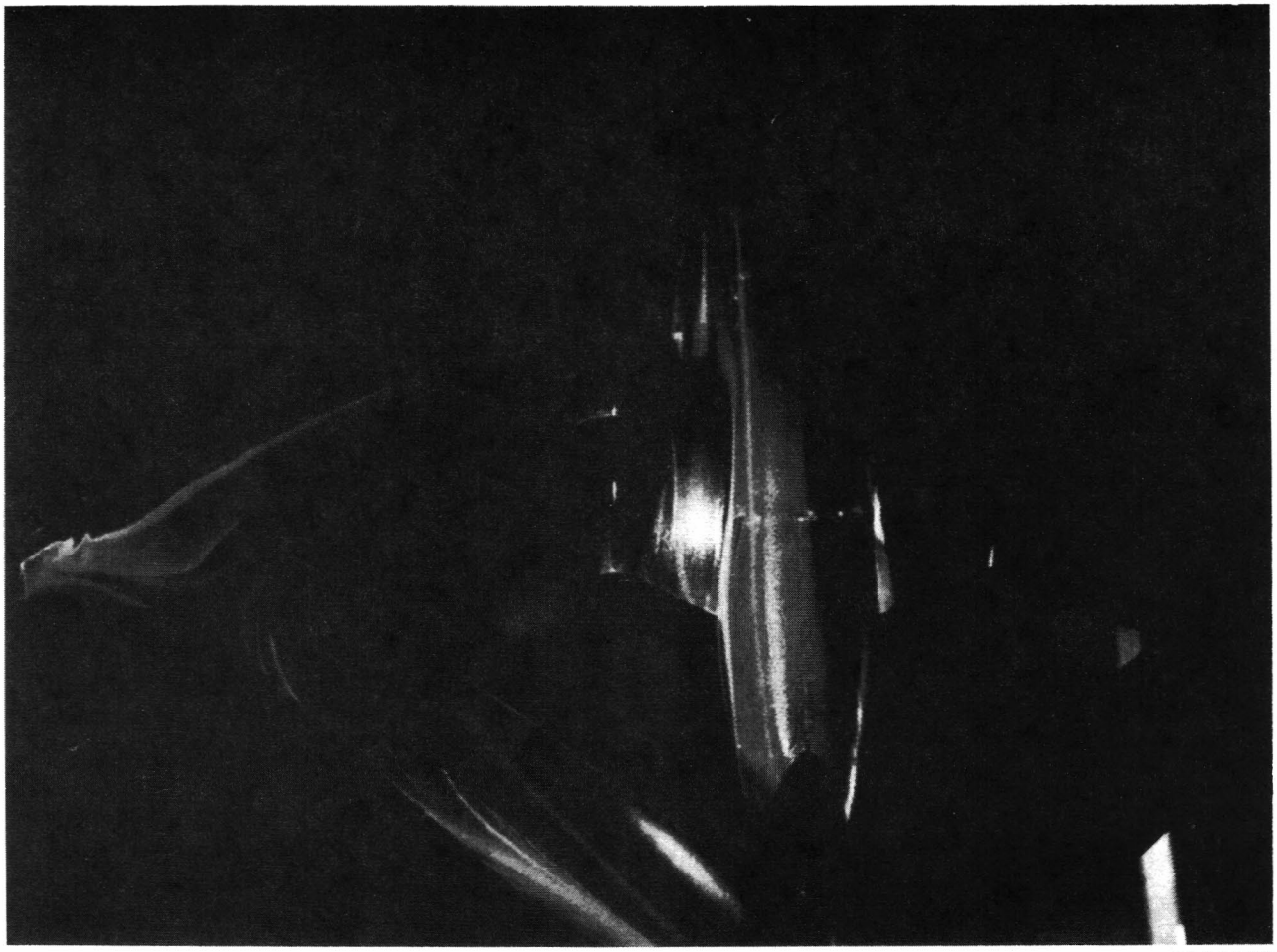

spb-3-9-jw-C2

Figure 6. Experimental Oil Flow Visualization at $M_\infty = 0.38$, $\alpha = 4°$ and $\beta = 0°$

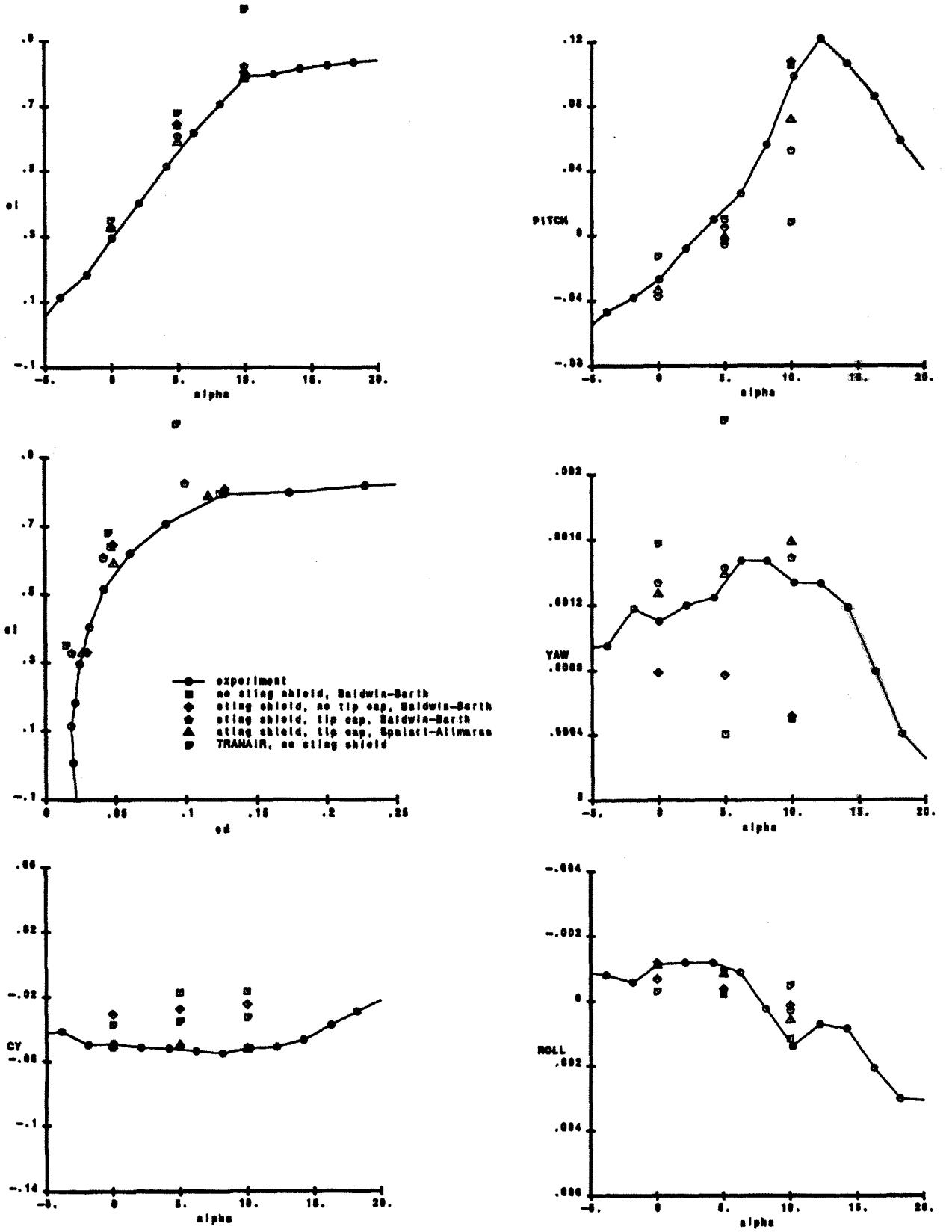

spb-3-9-jw-C4

Figure 7. Forces and Moments of Complete Configuration at $M_\infty = 0.30$ and $\beta = 5°$

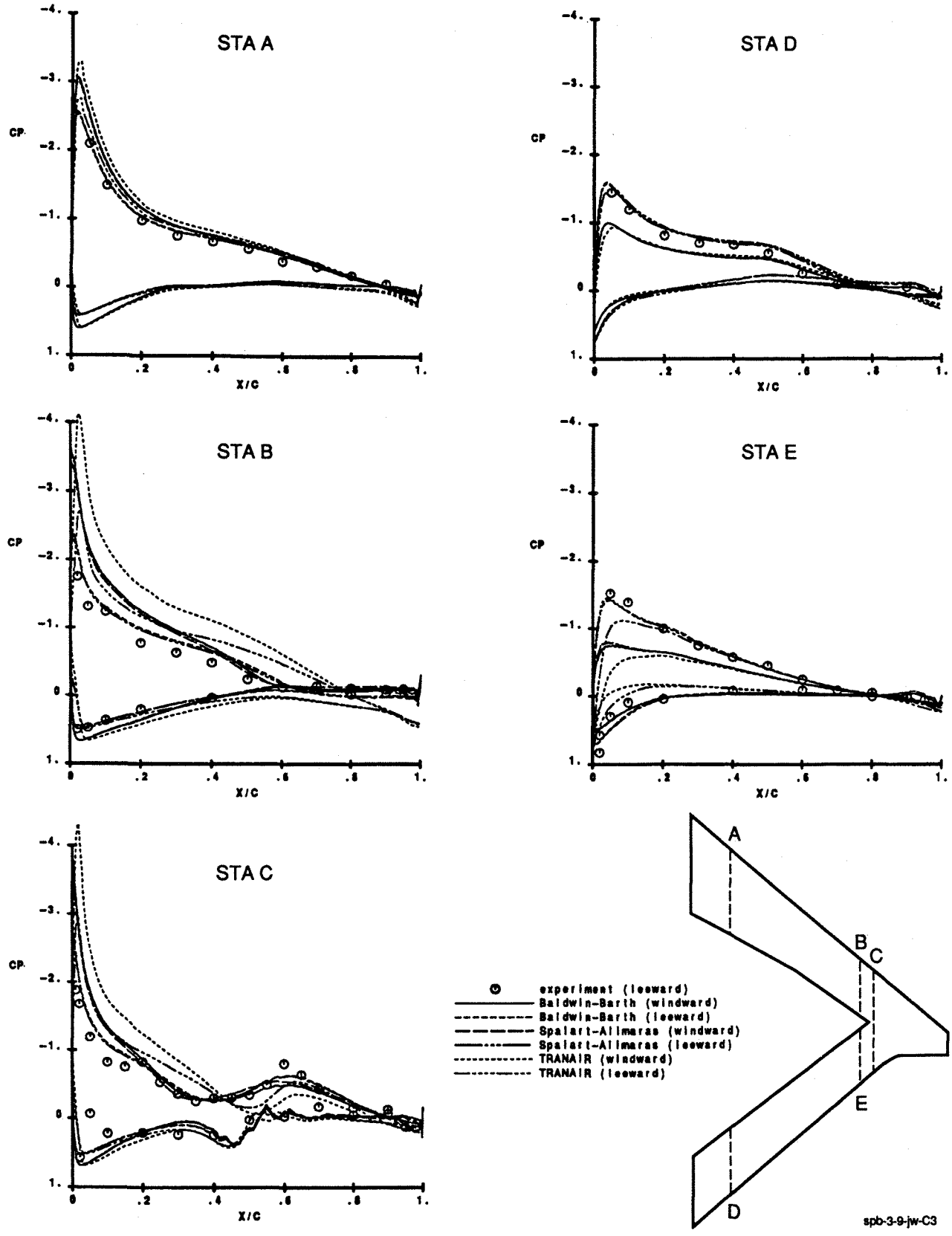

Figure 8. Comparison of Surface Pressure Distribution at $M_\infty = 0.30$, $\alpha = 5°$ and $\beta = 5°$